International Journal of Heat and Mass Transfer 52 (2009) 557–563

Contents lists available at ScienceDirect

International Journal of Heat and Mass Transfer

journal homepage: www.elsevier.com/locate/ijhmt

Heat transfer in all pipe flow regimes: laminar, transitional/intermittent, and turbulent

J.P. Abraham [a,*], E.M. Sparrow [b], J.C.K. Tong [b]

[a] Laboratory for Heat Transfer and Fluid Flow Practice, School of Engineering, University of St. Thomas, St. Paul, MN 55105-1079, USA
[b] Laboratory for Heat Transfer and Fluid Flow Practice, Department of Mechanical Engineering, University of Minnesota, Minneapolis, MN 55455-0111, USA

ARTICLE INFO

Article history:
Received 4 June 2008
Received in revised form 11 July 2008
Available online 31 August 2008

ABSTRACT

A predictive theory is presented which is capable of providing quantitative results for the heat transfer coefficients in round pipes for the three possible flow regimes: laminar, transitional, and turbulent. The theory is based on a model of laminar-to-turbulent transition which is also viable for purely laminar and purely turbulent flow. Fully developed heat transfer coefficients were predicted for the three regimes. The present predictions were brought together with the most accurate experimental data known to the authors as well as with several algebraic formulas which are purported to be able to provide fully developed heat transfer coefficients in the so-called transition regime between $Re = 2300$ and 10,000. It was found that over the range $Re > 4800$, both the present predictions and those of the Gnielinski formula [V. Gnielinski, New equations for heat and mass transfer in turbulent pipe and channel flow, Int. Chem. Eng. 16 (1976) 359–367] are very well supported by the experimental data. However, the Gnielinski model is less successful in the range from 2300 to 3100. In that range, the present predictions and those of Churchill [S. Churchill, Comprehensive correlating equations for heat, mass, and momentum transfer in fully developed flow in smooth tubes, Ind. Eng. Chem. Fundam. 16 (1977) 109–116] are mutually reinforcing. Heat transfer results in the development region have also been obtained. Typically, regardless of the Reynolds number, the region immediately downstream of the inlet is characterized by laminar heat transfer. After the breakdown of laminar flow, a region characterized by intermittent heat transfer occurs. Subsequently, the flow may become turbulent and fully developed or the intermittent state may persist as a fully developed regime. The investigation covered both of the basic thermal boundary conditions of uniform heat flux (UHF) and uniform wall temperature (UWT). In the development region, the difference between the respective heat transfer coefficients for the two cases was approximately 25% (UHF > UWT). For the fully developed case, the respective heat transfer coefficients are essentially equal in the turbulent regime but differ by about 25% in the intermittent regime. The reported results are for a turbulence intensity of 5% and flat velocity and temperature profiles at the inlet.

1. Introduction

A large number of heat exchangers operate in the so-called transition regime between laminar and turbulent flow. The need for information for the proper design of these devices has motivated several attempts to create algebraic relationships for the prediction of heat transfer coefficients at Reynolds numbers that lie in the range from 2300 to 10,000. All such predictive equations are based either on interpolations or curve fits to experimental data. Accurate experimental data in this range of Reynolds numbers are difficult to obtain, especially for gas flows where external heat losses may be as large as the heat flows to the fluid itself. This is because the heat transfer coefficients for the flowing gas are very small, so that the internal thermal resistance is appreciable compared to the external resistance. Furthermore, all the data used to develop the existing algebraic predictions are mean values rather than the fully developed values that are properly required for the development of the available algebraic predictions.

The main contributions to the literature for the algebraic prediction of heat transfer coefficients in the so-called transition regime are due to Kuznetsov and Leonencke [1] (as reported in [2]), Petersen and Christiansen [2], Gnielinski [3], Churchill [4], and Gnielinski [5]. The first two of these papers fitted an algebraic curve to experimental data for Prandtl numbers greater than two, but present an equation in which the Prandtl number is a freely prescribable parameter. In 1976, Gnielinski [3] modified the widely accepted Petukhov–Popov equation [6] which provides fully developed heat transfer coefficients for flows with Reynolds numbers exceeding 10,000. The thus-modified equation, which is purported to be applicable to Reynolds numbers as low as 2300, is compared

* Corresponding author. Tel.: +1 651 962 5766.
E-mail address: jpabraham@stthomas.edu (J.P. Abraham).

0017-9310/$ - see front matter © 2008 Elsevier Ltd. All rights reserved.
doi:10.1016/j.ijheatmasstransfer.2008.07.009

Nomenclature

a	transitional model constant
A	transitional model constant
c_p	specific heat
D	pipe diameter
E	model destruction terms
h	heat transfer coefficient
F_1, F_2	blending functions in SST model
k	thermal conductivity
Nu	Nusselt number
p	pressure
P	model production term
Pr	Prandtl number
q	heat flux
R	pipe radius
Re	Reynolds number based on pipe diameter
S	absolute value of the shear strain rate
T	temperature
u_i	local velocity
$\overline{U}$	average velocity
x_i	tensor coordinate direction

Greek symbols

α	thermal diffusivity
β_1, β_2	SST model constants
ω	specific rate of turbulence dissipation
μ	dynamic viscosity
κ	turbulent kinetic energy
Π	intermittency adjunct function
ν	kinematic viscosity
σ	Prandtl-like diffusivities
γ	intermittency
ρ	density
Θ	dimensionless temperature

Subscripts

bulk	fluid bulk quantity
eff	effective property
i, j	tensor notations
fd	fully developed
inlet	at pipe inlet
turb	turbulent
UHF	uniform heat flux
UWT	uniform wall temperature
wall	at the pipe wall
γ	intermittency
ω	specific rate of turbulence dissipation
Π	intermittency adjunct function

in [3] to an assemblage of experimental data taken over a multi-decade period and for a variety of operating conditions and fluids. It should be noted that the vast majority of the data were *mean* values of the heat transfer coefficient rather than fully developed values, reflecting the early era in internal convection investigations. The comparison of the Gnielinski equation with the data indicated a considerable amount of scatter, at least ±20%. This considerable scatter is likely due to the antiquity of the data and the absence of modern instrumentation.

The approach employed by Churchill [4] was to develop an interpolation formula for the Nusselt number between the limiting cases of laminar and fully turbulent flow. As with the other presently available algebraic predictive models, the Churchill contribution was based on available mean heat transfer information. More recently, Gnielinski [5] has provided an alternative approach to the prediction of heat transfer coefficients in the transition region based on a linear interpolation of the intermittency between the values of 0 and 1 between Re = 2300 and 10,000.

2. Numerical model

2.1. Conservation equations

The numerical model is built upon several sets of equations which describe the physical phenomena that underlie laminar, transitional, and turbulent flows. The first set of governing equations are the well-known Reynolds-averaged conservation equations for mass, momentum, and energy, which are written in tensor form as

$$\frac{\partial u_i}{\partial x_i} = 0 \tag{1}$$

$$\rho\left(u_i \frac{\partial u_j}{\partial x_i}\right) = -\frac{\partial p}{\partial x_i} + \frac{\partial}{\partial x_i}\left((\mu + \mu_{\text{turb}})\frac{\partial u_j}{\partial x_i}\right), \quad j = 1,2,3 \tag{2}$$

and

$$\rho c_p\left(u_i \frac{\partial T}{\partial x_i}\right) = \frac{\partial}{\partial x_i}\left(k_{\text{eff}} \frac{\partial T}{\partial x_i}\right) \tag{3}$$

These equations will be applied to all three flow regimes by making use of two sets of supplementary equations.

In Eq. (2), the quantity μ_{turb} is readily identified as the turbulent viscosity. In the energy equation, Eq. (3), the effective thermal conductivity k_{eff} represents contributions from the molecular conductivity k and the turbulent thermal conductivity k_{turb}. The turbulent thermal conductivity is quantified by means of the turbulent Prandtl number, which is defined as

$$Pr_{\text{turb}} = \frac{c_p \mu_{\text{turb}}}{k_{\text{turb}}} \tag{4}$$

With this definition, the effective thermal conductivity is rewritten as

$$k_{\text{eff}} = k + k_{\text{turb}} = \left(\frac{k}{\rho c_p}\right)\rho c_p + \frac{c_p \mu_{\text{turb}}}{Pr_{\text{turb}}} = \left(\frac{k}{\rho c_p} + \frac{\nu_{\text{turb}}}{Pr_{\text{turb}}}\right)\rho c_p \tag{5}$$

The first term in the parenthesis of the rightmost member of Eq. (5) is the molecular thermal diffusivity, α. The combination of Eqs. (4) and (5) yields the operating equation for thermal energy transport

$$\left(u_i \frac{\partial \Theta}{\partial x_i}\right) = \frac{\partial}{\partial x_i}\left(\left(\alpha + \frac{\nu_{\text{turb}}}{Pr_{\text{turb}}}\right)\frac{\partial \Theta}{\partial x_i}\right) \tag{6}$$

In this equation, Θ is a dimensionless temperature whose definition depends on the thermal situation being considered. For the case of prescribed surface temperature at a value T_{wall} and an inlet fluid temperature T_{inlet}, the definition of Θ is

$$\Theta \equiv \frac{T - T_{\text{inlet}}}{T_{\text{wall}} - T_{\text{inlet}}} \tag{7}$$

Alternatively, for uniform heat flux q at the bounding wall, the definition is

$$\Theta \equiv \frac{T - T_{\text{inlet}}}{(qR/k)} \tag{8}$$

Aside from the fluid properties ρ, μ, and α, which can be regarded as known, Eqs. (2) and (6) contain the special unknowns μ_{turb} and Pr_{turb}. The methods used to determine these quantities will be detailed in the following sections.

2.2. SST model for kinetic energy and specific dissipation rate

The turbulent flow will be determined using the SST model of Menter [7] which is conveyed in Eqs. (9) and (10). There, ω is the specific rate of turbulence dissipation, P_κ is the rate of production of the turbulent kinetic energy κ, and the terms σ_κ, σ_ω, and $\sigma_{\omega 2}$ are Prandtl number-like parameters for the transport κ and ω. Furthermore, F_1 is a blending function that facilitates the combination of the standard κ–ε model and the Wilcox κ–ω model [8,9]. The term S is the absolute value of the shear strain rate, and the β terms are model constants.

The factor γ, which multiplies the production term P_κ in Eq. (9) is worthy of special note. In the standard SST model, γ does not appear. Its role in Eq. (9) is to diminish the rate of turbulence production in flows that are not fully turbulent. The values of γ range between 0 and 1.

$$\frac{\partial(\rho u_i \kappa)}{\partial x_i} = \gamma \cdot P_\kappa - \beta_1 \rho \kappa \omega + \frac{\partial}{\partial x_i}\left[\left(\mu + \frac{\mu_{\text{turb}}}{\sigma_\kappa}\right)\frac{\partial \kappa}{\partial x_i}\right] \tag{9}$$

and

$$\frac{\partial(\rho u_i \omega)}{\partial x_i} = A\rho S^2 - \beta_2 \rho \omega^2 + \frac{\partial}{\partial x_i}\left[\left(\mu + \frac{\mu_{\text{turb}}}{\sigma_\omega}\right)\frac{\partial \omega}{\partial x_i}\right] + 2(1-F_1)\rho \frac{1}{\sigma_{\omega 2}\omega}\frac{\partial \kappa}{\partial x_i}\frac{\partial \omega}{\partial x_i} \tag{10}$$

The solution of Eqs. (9) and (10) yields the values of κ and ω, which are then used to evaluate the turbulent viscosity μ_{turb} from

$$\mu_{\text{turb}} = \frac{a\rho\kappa}{\max(a\omega, SF_2)} \tag{11}$$

in which F_2 is a function that limits the values of the turbulent viscosity in the near-wall region, a is a constant, and S has already been defined in connection with Eq. (10). Further details of the SST model can be found in [7].

2.3. Transition model

A transition model is needed to adapt the SST turbulence model to non-fully turbulent flows. This adaptation is achieved via the damping factor γ which appears in Eq. (9). As used here, γ is called the intermittency. It is not the same as the intermittency encountered in the prior literature. That intermittency was used to indicate the fraction of time that the flow at a specific location is turbulent.

Recent developments of a viable transition model may be traced to the work of Suzen and Menter. In a series of papers, Suzen and co-workers presented a one-equation model for the intermittency as a supplement of the shear stress transport (SST) turbulence model [10–13]. That intermittency factor was used as a multiplier of the SST-defined eddy viscosity. Although this approach was capable of yielding useful results, its structure was ill-suited for modern, multi-processor computational schemes. The difficulty is that it requires integrated boundary layer parameters for its implementation rather than local parameters. The capture of these integrated parameters cannot easily be performed in a parallel-processor environment.

The most current and readily implemented scheme for predicting transition and skin friction in *external flows* is that formulated by Menter and co-workers [14–16]. They devised a scheme in which two supplementary equations, one for the intermittency γ and the other for intermittency adjunct function Π, were employed in conjunction with the SST turbulence model. Two of the essential features of the Menter scheme are: (a) the intermittency controls (i.e., dampens) the rate of production of turbulence and (b) only local quantities appear in the formulation. It is relevant to note that the Menter intermittency factor differs from that of Suzen in that the latter used the intermittency as a multiplicative modifier of the eddy viscosity. Furthermore, the fact that only local quantities are used enables the Menter approach to be implemented on multi-processor computers. As with all eddy viscosity-based models, adjustable constants appear both in the constitutive equations as well as multipliers in the turbulence production and destruction terms. In the Menter model, the constants were determined by comparisons with experimental data for external flows.

The Menter model for external flows was recently adapted to internal flows in [17]. That adaptation was used to study the fluid flow characteristics of laminar, transitional/intermittent, and turbulent flows in round pipes. Here, the model of [17] is adapted to the heat transfer problem for the two basic thermal boundary conditions of uniform heat flux and uniform wall temperature.

To continue the analysis, an equation is needed for the determination of γ as it appears in Eq. (9). However, γ is dependent not only on the already-identified variables that are present in the preceding equations but also on a new variable Π which describes the local stability status of the flow in the near-wall region. The working equations for the intermittency and the intermittency adjunct function Π are

$$\frac{\partial(\rho\gamma)}{\partial t} + \frac{\partial(\rho u_i \gamma)}{\partial x_i} = P_{\gamma,1} - E_{\gamma,1} + P_{\gamma,2} - E_{\gamma,2} + \frac{\partial}{\partial x_i}\left[\left(\mu + \frac{\mu_{\text{turb}}}{\sigma_\gamma}\right)\frac{\partial \gamma}{\partial x_i}\right] \tag{12}$$

and

$$\frac{\partial(\rho\Pi)}{\partial t} + \frac{\partial(\rho u_i \Pi)}{\partial x_i} = P_{\Pi,t} + \frac{\partial}{\partial x_i}\left[\sigma_{\Pi,t}(\mu + \mu_{\text{turb}})\frac{\partial \Pi}{\partial x_i}\right] \tag{13}$$

The P quantities denote production of the respective dependent variables, and the E terms refer to destruction processes. Eqs. (1), (2), (6), (9), (10), (12), and (13) collectively constitute a coupled system of partial differential equations which yields velocities, pressure, temperature, turbulent kinetic energy, specific turbulent dissipation, and, in particular, the local state of transition conveyed by γ and Π.

2.4. Turbulent Prandtl number

The second special parameter that was identified in connection with Eq. (6) is the turbulent Prandtl number Pr_{turb}. Owing to its critical importance for the prediction of turbulent heat transfer, there exists an extensive literature describing various attempts to identify its magnitude. Perhaps the most definitive source of information about the turbulent Prandtl number is a review paper by Kays [18]. Among other issues, the paper indicates that values of the turbulent Prandtl number in the near-neighborhood of a wall can substantially exceed the traditional value of 0.9. In this regard, Crimaldi et al. [19] measured values of the turbulent Prandtl number as high as 10 for water flow. These reports of relatively high values of Pr_{turb} are reinforced by Bensayah et al. [20] and by Chua et al. [21] for heat transfer in jets. In atmospheric boundary layers, it was found by Grachev et al. [22] and by Bass et al. [23] that turbulent Prandtl numbers strongly depend on variations of the Richardson number and can reach values in excess of 40. Heat transfer measurements in a ribbed channel provided values of the turbulent Prandtl number of approximately 1.7 in a gas flow [24]. In this light, the information that was cited in the foregoing suggests the need to rethink the standard default treatment of the turbulent Prandtl number which is typically a value of 0.9.

In the present investigation, the choice of the values of the turbulent Prandtl number was made by comparing predictions of the fully developed Nusselt number with literature standards. The

fully developed heat transfer coefficient h_{fd} and Nusselt number Nu_{fd} are defined as

$$Nu_{fd} = \frac{h_{fd}D}{k}, \quad h_{fd} = \frac{q}{(T_{wall} - T_{bulk})}\bigg|_{fd} \tag{14}$$

To begin the aforementioned comparison, attention may be drawn to Fig. 1. That figure consists of two parts. The main part of the figure displays a large amount of *truly* fully developed experimental data for air flows in uniformly heated pipes [25–29], while the inset shows two popular algebraic correlations in the so-called transition regime. For the range of Reynolds numbers between 4800 and 40,000, the experimental data served as the standard of comparison to enable the turbulent Prandtl number to be chosen so that the predicted Nu_{fd} values are congruent with the data. The faired curve that appears in the main part of the figure is to provide continuity for the data.

Consideration of the most popular among the available algebraic correlations in the transition regime suggests some degree of insufficiency for both. The Gnielinski correlation [3] does not merge with the laminar results in a manner that would reinforce its acceptance for the lower Reynolds-number portion of the transition regime. On the other hand, while the Churchill correlation smoothly merges with the laminar regime, it clearly overestimates the experimental data at $Re = 4800$. Furthermore, its undulating behavior is inconsistent with rational expectations.

For the range of Reynolds numbers between 2300 and 4800, the turbulent Prandtl number determination was based on the Gnielinski [3] curve between the crossing-point Reynolds number of 3100 and 4800 and on the Churchill curve [4] for Reynolds numbers below 3100.

The values of the turbulent Prandtl numbers that resulted from the foregoing procedure are displayed in Fig. 2 where they are plotted as a function of the Reynolds number. There is a sharp peak whose onset is at $Re \sim 2300$ and which attains its maximum at about 2500. Thereafter, the values of the turbulent Prandtl number decrease, sharply at first, and then more gradually before achieving a constant value of 1.05. At the peak, Pr_{turb} equals 1.5. The Reynolds number range where the highest values of Pr_{turb} occur is unique in that very little prior investigation of its turbulence characteristics has been carried out. It is, clearly, a range in which the turbulence has a very different nature from that of a fully turbulent flow, so that information for the latter is likely to have little relevance for the former. From the foregoing literature survey, it was demonstrated that for situations that differ from those encountered in a fully developed pipe flow, values of Pr_{turb} in excess of one are not uncommon. It is believed that until further studies of the nature of turbulence which occurs just after laminar breakdown have been carried out, the values displayed in Fig. 2 should be considered as reasonable.

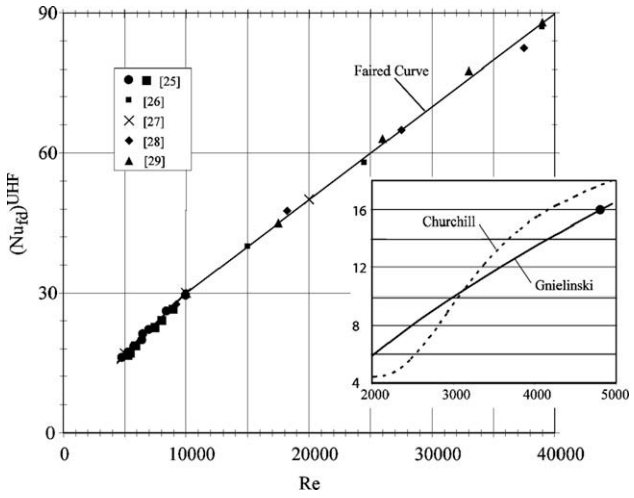

Fig. 1. Available fully developed experimental Nusselt-number data and algebraic curve fits used for the determination of the turbulent Prandtl number.

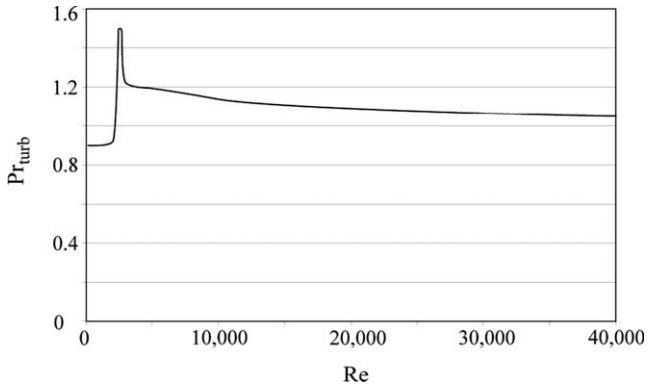

Fig. 2. Turbulent Prandtl numbers used in the present analysis for both UHF and UWT cases as a function of the Reynolds number.

It is worthy of note that the Pr_{turb} values exhibited in Fig. 2 were found to be applicable for both of the two investigated thermal boundary conditions, UHF and UWT. This insensitivity reinforces a similar independence of the turbulent Prandtl number on the thermal boundary conditions was noted by Churchill [30].

2.5. Numerical implementation

The first step in the implementation is the discretization of the solution domain. The solution domain was chosen to extend from the pipe inlet to a location 200 diameters downstream. The selection of this pipe length was made to ensure that fully developed conditions would be achieved. For the discretization, extreme care was taken to guarantee high accuracy of the solution in the neighborhood of the wall. In particular, the deployment of the elements was made so that the wall-adjacent element was displaced by a value $y^+ < 1.75$ at all axial locations and for all Reynolds numbers, so that numerous elements spanned the laminar sublayer which is widely regarded as being defined by $0 < y^+ < 5$. A mesh-independent study was performed which resulted in a mesh containing approximately 1,100,000 elements, with 50 elements spanning the cross section.

Boundary conditions at the inlet of the pipe require special consideration because of the uniqueness of some of the quantities that require specification. The value of the turbulence intensity Tu is sufficient to specify κ, ω, and Π. For the studies performed here, the inlet turbulence intensity was selected as 5%, which is typical for many pipe flows. Furthermore, although the inlet intermittency γ is set equal to 1 as a default value, it immediately drops to its natural value as dictated by the flow. The inlet axial velocity profile is uniform and is assigned a value which, in effect, specifies the Reynolds number of the flow. The other velocity components at the inlet are zero. Finally, for all cases, the dimensionless inlet temperature was assigned a value of 0.

At the downstream end of the solution domain, the streamwise second derivatives of all the dependent variables are zero, except for the pressure, for which a specified, area-averaged value is prescribed. At all bounding walls, the no-slip and impermeability conditions are enforced for all the velocity components. Also zero at the wall is the turbulence kinetic energy and the specific dissipation rate as well as the normal derivatives of both γ and Π. Two independent thermal conditions were employed at the walls. One condition was a dimensionless uniform heat flux (UHF), and the other was a dimensionless wall temperature (UWT). For the UHF

case, a dimensionless wall heat flux of 1 was applied, while for the UWT situation, a dimensionless wall temperature of 1 was employed.

The calculations were carried out using CFX 11.0, a commercial finite-volume-based CFD program. A false-transient, time-stepping approach is employed to enable convergence to the steady-state solution [31]. While the fully implicit, backward-Euler, time-stepping algorithm exhibits first-order accuracy in time, its use does not affect the accuracy of the final, converged solution.

Coupling of the velocity–pressure equations was achieved on a non-staggered, collocated grid using the techniques developed by Rhie and Chow [32] and Majumdar [33]. The inclusion of pressure-smoothing terms in the mass conservation equation suppresses oscillations which can occur when both the velocity and pressure are evaluated at coincident locations.

The advection terms in the momentum and energy equations were evaluated by using the upwind values of the momentum flux, supplemented with an advection-correction term. The correction term reduces the occurrence of numerical diffusion and is of second-order accuracy. Details of the advection treatment can be found in [34].

3. Results and discussion

3.1. Fully developed heat transfer results

The fully developed heat transfer results will be presented in terms of the fully developed Nusselt number whose definition was provided in Eq. (14). In the presentation of the results, Nu_{fd} is plotted as a function of the Reynolds number Re, which is

$$Re = \frac{\overline{U}D}{\nu} \tag{15}$$

The results will be shown in separate figures for the two boundary conditions, UHF and UWT. Fig. 3 conveys the UHF results predicted by the present model which are for $Pr = 0.70$. In addition to the present predictions, the figure contains experimental data for air flow from the same independent investigations that were already cited in connection with Fig. 1 [25–29]. The data correspond specifically to the fully developed state, in contrast to the mean Nusselt numbers which were used as the basis of previously existing algebraic representations.

The results conveyed in the figure cover the range of Reynolds numbers from 1100 to 40,000. It is relevant to note that all of the present predictions were based on the same transition model, even those for the pure laminar and pure turbulent regimes.

Next, the present predictions will be compared with the most popular of the algebraic predictions. The comparison is presented in Fig. 4 for Reynolds numbers ranging from 1100 to 40,000. The figure is subdivided into two parts, with the main part of the figure devoted to the range of Reynolds numbers from 1100 to 10,000 and the inset containing results for the range 10,000 to 40,000.

Focus is first directed to the main part of the figure. An overall view of the figure suggests that the correlations of [2,5] are not of practical use. The Gnielinski equation [3] is to be regarded as being valid for Reynolds numbers above 3100, while it appears that it should not be used for Reynolds numbers below that value. On the other hand, the Churchill correlation [4] provides a good bridge between the Reynolds numbers of 2300 and 3100. However, it appears that for Reynolds numbers above 3100, the Churchill correlation would not give accurate predictions. It is believed that the present predictions are valid over the entire range of Reynolds numbers of the figure.

The inset of Fig. 4 examines the low and intermediate turbulent Reynolds number range. It can be seen from the figure that the present predictions reinforce the Gnielinski equation [3]. The Petukhov–Popov correlation [6] is in somewhat lesser agreement with the present predictions, while the Churchill interpolation formula [4] deviates from the others. Since, as demonstrated in Fig. 3, the present predictions are an excellent representation of multiple, independently performed experiments, it appears to be a fair standard for the comparison with the main algebraic models.

The next issue to be considered is the difference in the fully developed Nusselt numbers for the basic boundary conditions of uniform heat flux and uniform wall temperature. That comparison is conveyed in Fig. 5 for Reynolds numbers up to 10,000. It can be seen from the figure that the deviations between the respective Nusselt number values are greatest in the laminar flow regime and diminish as the Reynolds number increases throughout the transition and low-Reynolds-number turbulent regimes. The laminar-flow Nusselt numbers of 3.66 and 4.36 correspond to a 17% deviation. For increasing Reynolds numbers, the deviation disappears at a Reynolds number of approximately 8000. Further calculations up to $Re = 40{,}000$ confirm the virtually perfect agreement between the Nusselt numbers for the two boundary conditions.

The equations which describe the present Nusselt number results for the UHF and UWT boundary conditions for the Reynolds number range between 2300 and 3100 are, respectively,

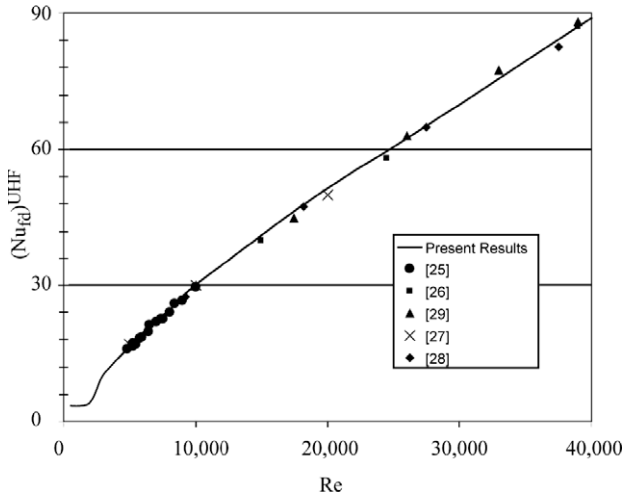

Fig. 3. Comparison of presently predicted fully developed *Nu* numbers for the uniform heat flux case with experimental data.

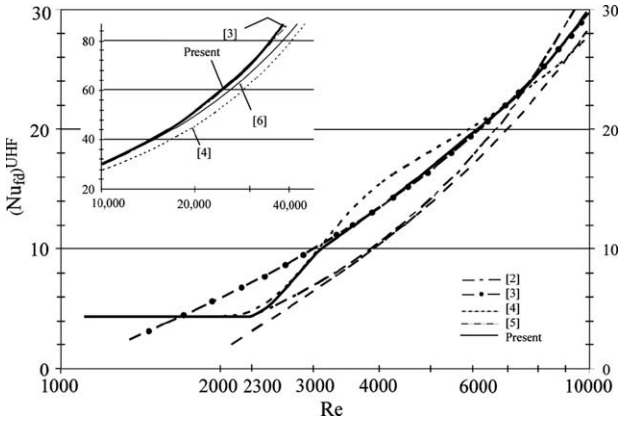

Fig. 4. Comparison of present predictions for fully developed Nusselt numbers for the uniform heat flux case with algebraic predictions from the literature.

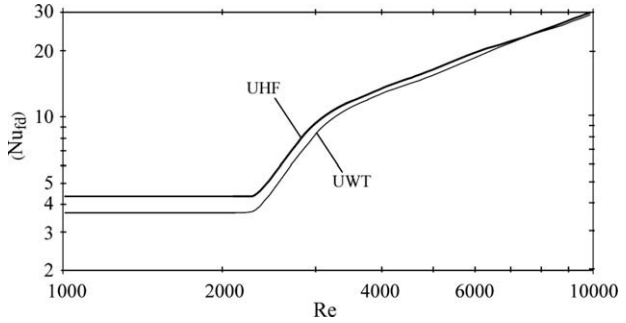

Fig. 5. Comparison of fully developed Nusselt numbers for the uniform heat flux (UHF) and uniform wall temperature (UWT) boundary conditions.

$$(Nu_{fd})_{UHF} = 3.5239\left(\frac{Re}{1000}\right)^4 - 45.148\left(\frac{Re}{1000}\right)^3 + 212.13\left(\frac{Re}{1000}\right)^2 - 427.45\left(\frac{Re}{1000}\right) + 316.08 \quad (16a)$$

$$(Nu_{fd})_{UWT} = 2.2407\left(\frac{Re}{1000}\right)^4 - 29.499\left(\frac{Re}{1000}\right)^3 + 142.32\left(\frac{Re}{1000}\right)^2 - 292.51\left(\frac{Re}{1000}\right) + 219.88 \quad (16b)$$

For $Re > 3100$, it is suggested that the Gnielinski formula [3] be used for both boundary conditions.

3.2. Local heat transfer results

Attention will now be turned to the local Nusselt number and its variation in the streamwise direction. Results corresponding to the UHF boundary condition are presented in Fig. 6. The figure contains a succession of curves which are parameterized by the Reynolds number over the range 1670 to 40,000. The results are extended over the x/D range from 0 to 200. As can be seen from the figure, it is clear that a number of fluid flow phenomena are reflected in the shapes of the curves. In all cases, starting at the inlet, the local Nusselt number decreases sharply until a minimum is achieved for cases where $Re > 2300$. The minimum can be identified with the breakdown of laminar flow. The rate of descent of the Nusselt number is a strong function of the Reynolds number. In particular, at the lower $Re > 2300$, the decrease is gradual and a plateau-like shape is achieved. With increasing Reynolds number, the descent becomes much steeper and the plateau vanishes. Thereafter, the Nusselt number increases and eventually reaches a constant value which can be identified as the fully developed state.

The penetration of the laminar region into the pipe is largest at the lower Reynolds numbers and shrinks as the Reynolds number increases. Furthermore, the attainment of fully developed heat transfer requires a greater length at the lower $Re > 2300$. This length also diminishes with increasing Reynolds number.

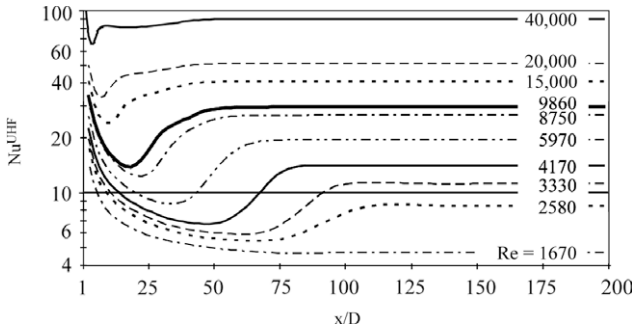

Fig. 6. Axial distribution of the local Nusselt number for the UHF case.

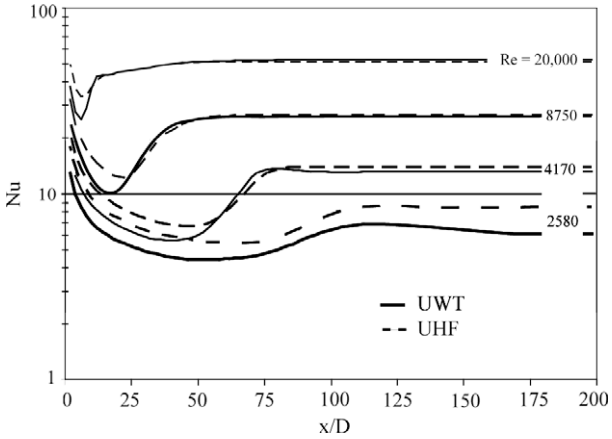

Fig. 7. Comparison of local Nusselt numbers for the UHF and UWT cases.

The curve for $Re = 1670$ is illustrative of the Nusselt number development for all laminar flow Reynolds numbers. In those cases, it is clear that the initial descent of the Nusselt number is slower than those for the $Re > 2300$ cases. Not unexpectedly, the local Nusselt numbers for the laminar cases merge monotonically with those for the fully developed state.

Further observation of Fig. 6 enables the identification of the point of laminar breakdown. If breakdown is associated with the minimum value of the Nusselt number, it is seen that for the cases covered in the figure, breakdown ranges from approximately 70 diameters to 4 diameters as the Reynolds number ranges from 2580 to 40,000. Although it is clear that laminar flow persists only for short distances into pipes when the Reynolds number is high, it is noteworthy that there is such a laminar region. This finding reinforces the original observations of Osborne Reynolds in 1883 [35]. In those experiments, performed as a flow visualization by means of a dye stream in water, Reynolds found that the onset of turbulence in a pipe always occurred downstream of the inlet. In the region between the inlet and the onset of turbulence, laminar flow existed.

The final presentation will continue the focus on local Nusselt numbers but will encompass both of the thermal boundary conditions, UHF and UWT. Fig. 7 conveys a comparison of the axially developing local Nusselt numbers for these cases and for a selected set of Reynolds numbers. It can be seen from the figure that in the developing portion of the Nusselt number distribution, the UHF values always exceed those for UWT. This behavior can be attributed to the laminar nature of the initial portion of the development region. In the region of thermally developed conditions, there is a distinct difference between the results for the two boundary conditions when the Reynolds number is relatively low. Again, this finding is consistent with the laminar relationship between the two types of boundary conditions. With increasing Reynolds number, however, the fully developed Nusselt numbers tend to merge to a common value.

4. Concluding remarks

This investigation has had several foci, all of which are related to the quantitative prediction of heat transfer in all the possible regimes that occur when fluid flows in a straight pipe. A model for the transition of the flow from laminar-to-intermittent-to-turbulent has been adopted for this purpose. This model is applicable for pure laminar flow, intermittent flow, and for fully turbulent flow. In particular, it can be used to predict heat transfer coeffi-

cients either in the development region or the fully developed region for each of these flow regimes. In addition to the well-known fully developed regimes for laminar and turbulent flow, the present work has identified a third fully developed regime which may be characterized as fully developed intermittent.

For the fully developed regimes, attention has been focused not only on the present predictions, but on the available algebraic formulae which are purported to provide information about fully developed heat transfer in the so-called transition regime which is commonly assumed to extend between $Re = 2300$ and $Re = 10{,}000$. In addition, definitive experimental data have been identified and are used to test the present predictions and those of the algebraic formulae. It was found that both the Gnielinski [3] formula and the present predictions are supported by the experimental data in the range $Re > 4800$. The evaluation of the Gnielinski formula for lower Reynolds numbers leads to the conclusion that there is a range of Reynolds numbers between 2300 and 3100 for which its accuracy is questionable. On the other hand, both the present results and the algebraic formula due to Churchill [4] appear to adequately bridge the aforementioned gap and smoothly mate with the laminar results. On the basis of the presented results, it is believed that the present predictions are valid for all Reynolds numbers.

The variation of the local heat transfer coefficients along the length of the pipe has been determined as well as the fully developed values. In the near-inlet region, the flow is laminar. Subsequent to the breakdown of laminar flow, a region of intermittency is present. This intermittency may either evolve into a fully turbulent flow or may, alternatively, become a fully developed intermittent flow. Quantitative information in the form of local Nusselt numbers is presented for all of these cases.

The two basic boundary conditions, uniform heat flux and uniform wall temperature, give rise to local heat transfer coefficients in the development region that differ by about 25%. However, for fully developed turbulent flow, the heat transfer coefficients for the two cases are virtually coincident. If, on the other hand, the fully developed regime is intermittent, the two boundary conditions give rise to values of the heat transfer coefficient which differ by approximately 25%.

Acknowledgement

Support of H. Birali Runesha and the Supercomputing Institute for Digital Simulation & Advanced Computation at the University of Minnesota is gratefully acknowledged.

References

[1] M.D. Kuznetsov, V.M. Leonencke, Khim. Nauka Prom. 4 (1959) 406 .
[2] A. Petersen, E. Christiansen, Heat transfer to non-Newtonian fluids in transitional and turbulent flow, AIChE J. 12 (1966) 221–231.
[3] V. Gnielinski, New equations for heat and mass transfer in turbulent pipe and channel flow, Int. Chem. Eng. 16 (1976) 359–367.
[4] S. Churchill, Comprehensive correlating equations for heat, mass, and momentum transfer in fully developed flow in smooth tubes, Ind. Eng. Chem. Fundam. 16 (1977) 109–116.
[5] V. Gnielinski, Heat Exchanger Design Handbook, Chapter 5, Single-Phase Convective Heat Transfer: Forced Convection in Ducts, Heat Exchanger Design Updates, Begell House, 1999.
[6] B. Petukhov, V. Popov, Theoretical calculations of heat exchange and frictional resistance in turbulent flow in tubes of an incompressible fluid with variable physical properties, High Temp. 1 (1963) 69–83.
[7] F. Menter, Two-equation eddy-viscosity turbulence models for engineering applications, AIAA J. 32 (1994) 1598–1605.
[8] D. Wilcox, Reassessment of the scale-determining equation for advanced turbulence models, AIAA J. 26 (1988) 1299–1310.
[9] D. Wilcox, Comparison of two-equation turbulence models for boundary layers with pressure gradient, AIAA J. 31 (1994) 1414–1421.
[10] Y. Suzen, P. Huang, Modeling of flow transition using an intermittency transport equation, J. Fluids Eng. 122 (2000) 273–284.
[11] Y. Suzen, G. Xiong, P. Huang, Predictions of transitional flows in low-pressure turbines using intermittency transport equation, AIAA J. 42 (2002) 254–266.
[12] Y. Suzen, P. Huang, Predictions of separated and transitional boundary layers under low-pressure turbine airfoil conditions using an intermittency transport equation, J. Turbomach. 125 (2003) 455–464.
[13] Y. Suzen, P. Huang, Comprehensive Validation of an Intermittency Transport Model for Transitional Low-Pressure Turbine Flows, 42nd Aerospace Sciences Meeting and Exhibit, Reno, NV, January 5–8, 2004.
[14] F. Menter, T. Esch, S. Kubacki, Transition modelling based on local variables, in: Fifth International Symposium on Engineering Turbulence Modeling and Measurements, Mallorca, Spain, 2002.
[15] F. Menter, R. Langtry, S. Likki, Y. Suzen. P. Huang, S. Volker, A correlation-based transition model using local variables, Part I – Model formulation, in: Proceedings of ASME Turbo Expo Power for Land, Sea, and Air, Vienna, Austria, June 14–17, 2004.
[16] F. Menter, R. Langtry, S. Likki, Y. Suzen, P. Huang, S. Volker, A correlation-based transition model using local variables, Part II – Test cases and industrial applications, in: Proceedings of ASME Turbo Expo Power for Land, Sea, and Air, Vienna, Austria, June 14–17, 2004.
[17] J. Abraham, E. Sparrow, J. Tong, Breakdown of laminar pipe flow into transitional intermittency and subsequent attainment of fully developed intermittent or turbulent flow, Numer. Heat Transfer 54 (2008) 103–115.
[18] W. Kays, Turbulent Prandtl number – where are we?, J Heat Transfer 116 (1994) 284–295.
[19] J. Crimaldi, J. Koseff, S. Monismith, A mixing-length formulation for the turbulent Prandtl in wall-bounded flows with bed roughness and elevated scalar sources, Phys. Fluids 18 (2006) 095102.
[20] K. Bensayah, A. Benchatti, M. Aouissi, A. Bounif, Scalar turbulence model investigation with variable turbulent Prandtl number applies in hot axisymmetric turbulent round jet, Heat Tech. 25 (2007) 49–56.
[21] L. Chua, Y. Li, T. Zhou, Measurements of a heated square jet, AIAA J. 42 (2004) 578–588.
[22] A. Grachev, E. Andreas, C. Fairall, P. Guest, O. Persson, On the turbulent Prandtl number in the stable atmospheric boundary layer, Boundary-Layer Meteorol. 125 (2007) 329–341.
[23] P. Bass, S. de Roode, G. Lenderink, The scaling behaviour of a turbulent kinetic energy closure model for stably stratified conditions, Boundary-Layer Meteorol. 127 (2008) 17–36.
[24] S. Jenkins, J. Con Wolfersdorf, B. Weigand, T. Roediger, H. Knauss, E. Kraemer, Time-Resolved Heat Transfer Measurements on the Tip Wall of a Ribbed Channel Using a Novel Heat Flux Sensor – Part II: Heat Transfer Results, ASME Turbo Expo 2006, Power for Land, Sea, and Air, Barcelona, Spain, May 6–11, 2006.
[25] S. Lau, Effect of Plenum Length and Diameter on Turbulent Heat Transfer in a Downstream Tube and on Plenum-Related Pressure Loss, PhD Thesis, University of Minnesota, 1980.
[26] L. Bosmans, Effect of Nonaligned Plenum Inlet and Outlet on Heat Transfer in a Downstream Tube and on Pressure Drop, MS Thesis, University of Minnesota, 1981.
[27] R. Kemink, Heat Transfer in a Tube Downstream of a Fluid Withdrawal Branch, MS Thesis, University of Minnesota, 1977.
[28] D. Wesley, Heat Transfer in a Pipe Downstream of a Tee, PhD Thesis, University of Minnesota, 1976.
[29] A. Black III, The Effect of Circumferentially-Varying Boundary Conditions on Turbulent Heat Transfer in a Tube, PhD Thesis, University of Minnesota, 1966.
[30] S. Churchill, A reinterpretation of the turbulent Prandtl number, Ind. End. Chem. Res. 41 (2002) 6393–6401.
[31] CFX Version 11.0 Manual, ANSYS, Inc, Canonsburg, PA.
[32] C. Rhie, W. Chow, A Numerical Study of the Turbulent Flow Past an Isolated Airfoil with Trailing Edge Separation, AIAA Paper No. 82-0998, 1982.
[33] S. Majumdar, Role of underrelaxation in momentum interpolation for calculation of flow with nonstaggered grids, Numer. Heat Transfer 13 (1988) 125–132.
[34] T. Barth, D. Jesperson, The Design and Applications of Upwind Schemes on Unstructured Meshes, AIAA Paper No. 89-03, 1989.
[35] O. Reynolds, An experimental investigation of the circumstances which determine whether the motion of water shall be direct or sinuous, and of the law of resistance in parallel channels, Philos. Trans. R. Soc. Lond. 174 (1883) 935–982.